

Contents list available at **IJND**  
**International Journal of Nano Dimension**

Journal homepage: [www.IJND.ir](http://www.IJND.ir)

## Structural characterization of ZnO and ZnO:Mn nanoparticles prepared by reverse micelle method

### ABSTRACT

**M. Mazhdi\***

**P. Hossein Khani**

*Department of Physics, Faculty of Sciences, I.H.U, Tehran, Iran.*

Received: 15 June 2011

Accepted: 28 August 2011

In this article, ZnO and ZnO:Mn nanoparticles prepared by reverse micelle method. The various crystalline properties of these nanoparticles such as size, d-spacing, strain, stress, dislocation density and texture coefficient have been calculated with the help of XRD spectrum. The XRD results indicated that the synthesized ZnO and ZnO:Mn nanoparticles have a pure wurtzite (hexagonal phase) structure. It can be seen that the highest texture coefficient was in (002) plan for nanoparticles. The optical band gap energy of ZnO and ZnO:Mn nanoparticles have been analyzed by using UV-Vis data. The photoluminescence spectra of the nanoparticles indicated their high structural and optical quality.

**Keywords:** *ZnO; Nanoparticles; Reverse micelle, Structural properties; Photoluminescence.*

### INTRODUCTION

Semiconductor nanoparticles have attracted great applied during the past two decades. New devices with semiconductor nanoparticles may possess novel optical and electronic properties, which are potentially useful for technological applications, compared to the corresponding bulk materials [1-3]. Extremely high surface area to volume ratio is obtained with the decrease of particle size, which leads to an increase in surface specific active sites for chemical reactions and photon absorptions. The enhanced surface area also affects chemical reaction dynamics. The size quantization increases the energy band gap between the conduction band electrons and valence band holes which leads to change in their optical properties [3]. Zinc oxide, a typical II–VI compound semiconductor, with a direct band gap of 3.2 eV at room temperature and 60 meV as excitonic binding energy, is a very good luminescent material used in displays, ultraviolet and visible lasers, solar cells components, gas sensors and varistors [1,3].

\* Corresponding author:

Meysam Mazhdi

Department of Physics, Faculty of Sciences, I.H.U, Tehran, Iran.

Tel +98 2177104932

Fax +98 2177104938

Email [meisam.physics@gmail.com](mailto:meisam.physics@gmail.com)

Recently, a number of techniques such as reverse micelle, hydrothermal, sol-gel, and wet chemical have been employed in the synthesis of zinc oxide nanoparticles [1-4]. However, the reverse micelle technique is one of the more widely recognized methods due to its several advantages, for instance, soft chemistry, demanding no extreme pressure or temperature control, easy to handle, and requiring no special or expensive equipment [4]. In this scientific work, ZnO and ZnO:Mn nanoparticles were fabricated through the reverse micelle method. The structural and optical characteristics of these nanoparticles were analyzed.

## EXPERIMENTAL

### Preparation

ZnO and ZnO:Mn nanoparticles were fabricated through the mixture of two microemulsion systems. In microemulsion (I) butanol as oil, PVP as surfactant and zinc acetate (or zinc acetate and 1% by weight manganese acetate for ZnO:Mn nanoparticles) and water as aqueous phase were used in solution. Microemulsion (II) has similar mixture but instead of previous aqueous solution, the potassium hydroxide and water were used as aqueous media. The two microemulsion solutions (I) and (II) were mixed vigorously with a magnetic stirrer. Then centrifugation took place and the precipitation was kept at 250°C for 3 hours, till ZnO and ZnO:Mn nanoparticles were fabricated.

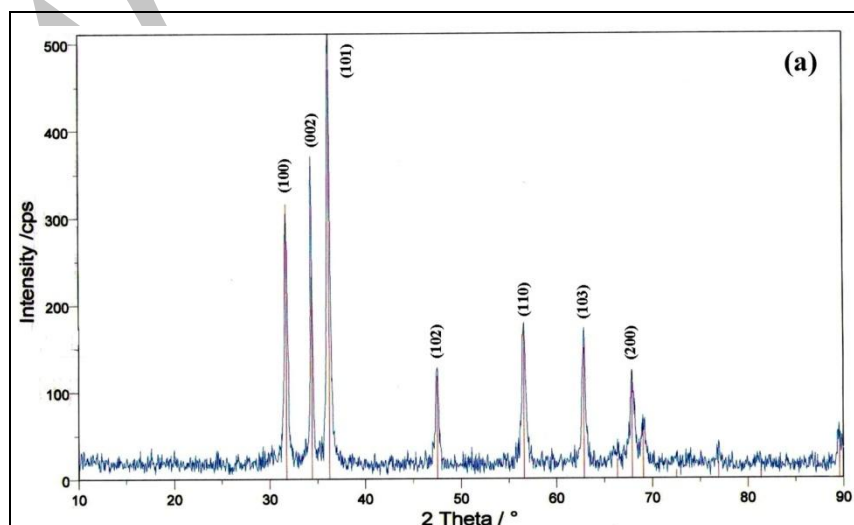
### Characterization

Obtained nanoparticles were analyzed by X-ray diffractometer (Scifert, 3003 TT) with Cu- $k_{\alpha}$  radiation, UV-Vis spectrometer (PERKIN ELMER, Lambda 45), luminescence spectrophotometer (PERKIN ELMER, LF55) and Atomic absorption spectrometer (PERKIN ELMER, 1100B).

## RESULTS AND DISCUSSION

### XRD analysis

Figure 1 shows the XRD patterns of ZnO and ZnO:Mn nanoparticles. The spectrums show three broad peaks for ZnO and ZnO:Mn at the  $2\theta=31.744, 34.398, 36.223$  and  $2\theta=31.647, 34.313, 36.131$  positions. The three diffraction peaks correspond to the (100), (002), and (101) crystalline planes of hexagonal ZnO. All the peaks in the XRD patterns of ZnO and ZnO:Mn samples could be fitted with the hexagonal wurtzite structure having slightly increased lattice parameter values for Mn doped sample (For ZnO nanoparticles  $a = 3.250 \text{ \AA}$ ,  $c = 5.207 \text{ \AA}$  and ZnO:Mn nanoparticles,  $a = 3.256 \text{ \AA}$ ,  $c = 5.212 \text{ \AA}$ ) in comparison to that of pristine ZnO sample ( $a = 3.249 \text{ \AA}$ ,  $c = 5.205 \text{ \AA}$ ) (JCPDS no. 36-1451). The increased lattice parameter values of Mn doped ZnO indicates the incorporation of Mn at Zn sites [4]. The broadening of the XRD lines is attributed to the nanocrystalline characteristics of the samples, which indicates that the particle size is in nanometer range.



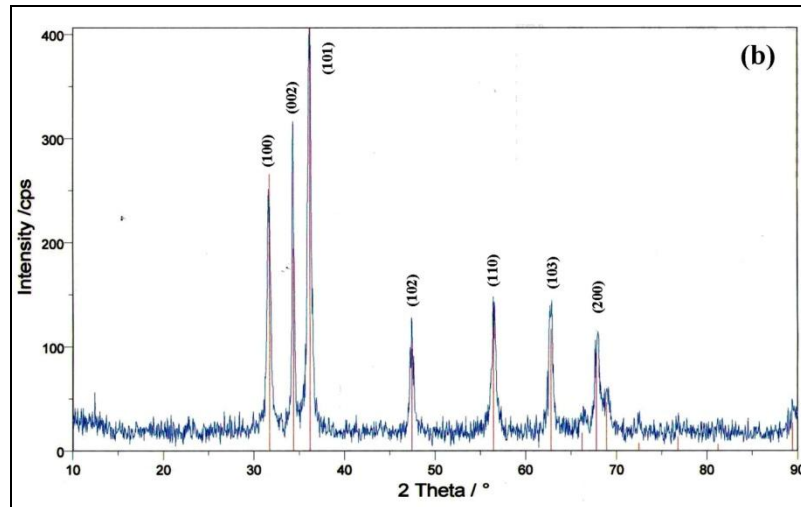


Fig. 1. XRD patterns of ZnO (a) and ZnO:Mn (b) nanoparticles.

The inter planar spacing ( $d$ ) is evaluated using the relation (1),

$$\frac{1}{d^2} = \frac{4}{3} \left( \frac{h^2 + hk + k^2}{a^2} \right) + \frac{l^2}{c^2} \quad (1)$$

$d$ -spacing for (100), (002), (101) planes is 2.8146, 2.6035, 2.4760 Å and 2.8204, 2.6062, 2.4806 Å for ZnO and ZnO:Mn nanoparticles, respectively. But, due to the size effect, the XRD peaks are broad. From the width of the XRD peak broadening, the mean crystalline size has been calculated using Scherer's equation [5]:

$$D = \frac{K\lambda}{\beta \cos \theta} \quad (2)$$

Where  $D$  is the diameter of the particle,  $K$  is a geometric factor taken to be 0.9,  $\lambda$  is the X-ray wavelength,  $\theta$  is the diffraction angle and  $\beta$  is the full width at half maximum of the diffraction main peak at  $2\theta$ . The mean crystal size of ZnO and ZnO:Mn nanoparticles resulted to be 21 and 18 nm. Quantitative information concerning the preferential crystal orientation can be obtained from the texture coefficient,  $TC$ , defined as [6],

$$TC = \frac{I(hkl)}{I_0(hkl)} \bigg/ \frac{1}{n} \sum_n \frac{I(hkl)}{I_0(hkl)} \quad (3)$$

Where  $TC(hkl)$  is the texture coefficient,  $I(hkl)$  is the XRD intensity and  $n$  is the number of diffraction peaks considered.  $I_0(hkl)$  is the intensity of the XRD reference of the randomly oriented grains. If  $TC(hkl) \approx 1$  for all the  $(hkl)$  planes considered, then the nanoparticles are with a randomly oriented crystallite similar to the JCPDS reference, while values higher than 1 indicate the abundance of grains in a given  $(hkl)$  direction. Values  $0 < TC(hkl) < 1$  indicate the lack of grains oriented in that direction. As  $TC(hkl)$  increases, the preferential growth of the crystallites in the direction perpendicular to the  $hkl$  plane is greater. Since three diffraction peaks were used ((100), (002), (101)). It can be seen that the highest  $TC(hkl)$  was in (002) plane for ZnO and ZnO:Mn nanoparticles. We used the Williamson–Hall equation to calculate the strain and particle size of the samples. The Williamson–Hall equation is expressed as follows [5]:

$$\beta \cos \theta = \frac{k\lambda}{D} + 4\varepsilon \sin \theta \quad (4)$$

In this equation,  $\beta \cos \theta$  is plotted against  $\sin \theta$ . Using a linear extrapolation to this plot, the intercept gives the particle size  $k\lambda/D$  and the slope represents the strain ( $\varepsilon$ ) for ZnO and ZnO:Mn nanoparticles as shown in Figure 2. The internal lattice strain value was found to be  $1.46 \times 10^{-3}$  and  $1.41 \times 10^{-3}$  for ZnO and ZnO:Mn nanoparticles, respectively.

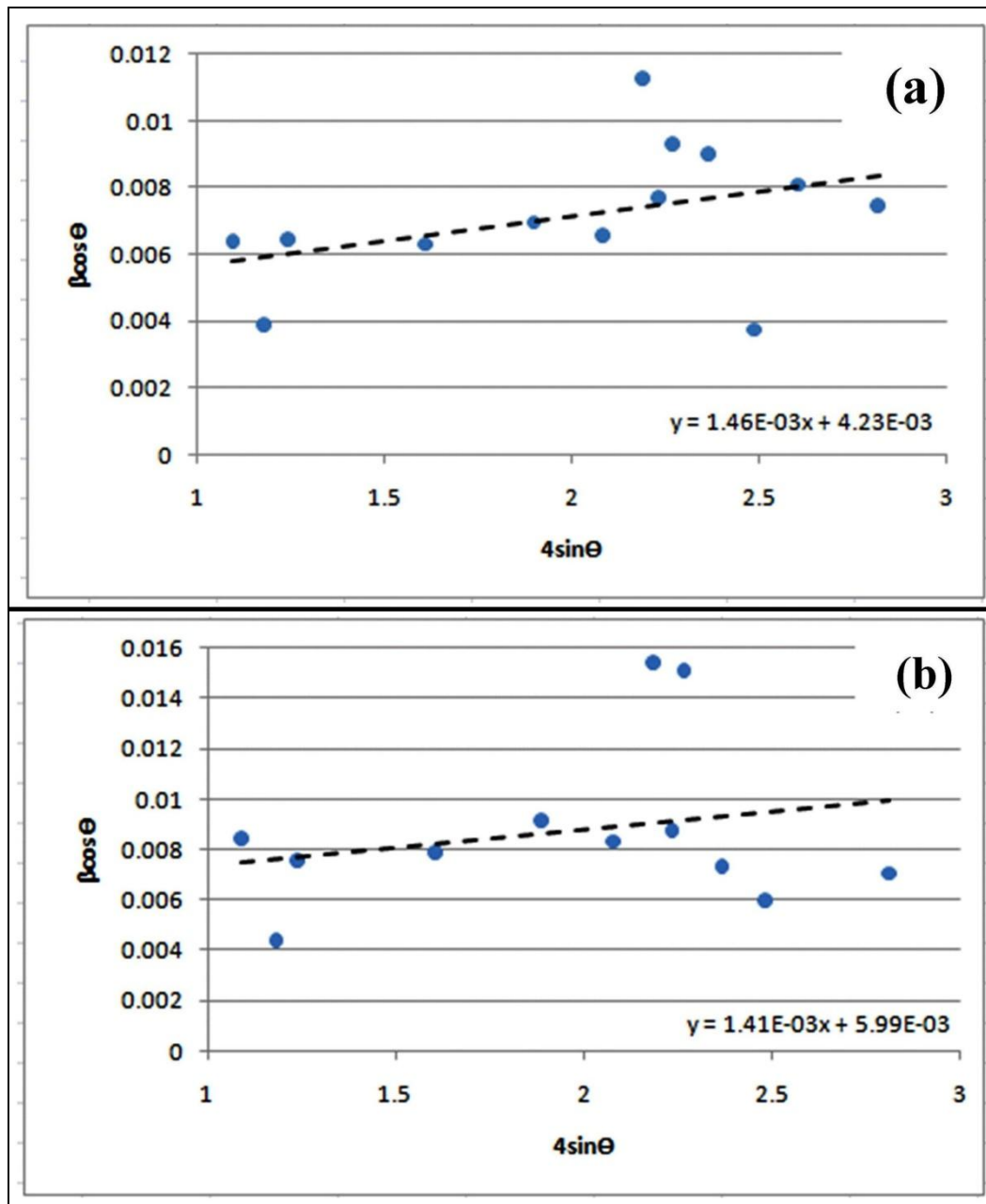


Fig. 2. The Williamson–Hall analysis for ZnO (a) and ZnO:Mn (b) nanoparticles. Strain is extracted from the slope.

Furthermore, the intrinsic stress ( $\zeta_s$ ) is calculated using the modified form of Williamson–Hall relation [5]:

$$\beta\cos\theta = \left(\frac{k\lambda}{D}\right) + \left(\frac{4\sigma\sin\theta}{Y}\right) \quad (5)$$

Where Y is the Young's modulus for ZnO (130GPa), D is the diameter of the particle, K

is a geometric factor,  $\lambda$  is the X-ray wavelength,  $\theta$  is the diffraction angle and  $\beta$  is the full width at half maximum of the diffraction peak at  $2\theta$  for nanoparticles. Plots were drawn with  $(4\sin\theta)/Y$  on the x-axis and  $\beta\cos\theta$  on the y-axis for the ZnO and ZnO:Mn nanoparticles as shown in Figure 3. The intrinsic stress ( $\zeta_s$ ) is calculated to be 189 and 183 MPa for ZnO and ZnO:Mn nanoparticles.

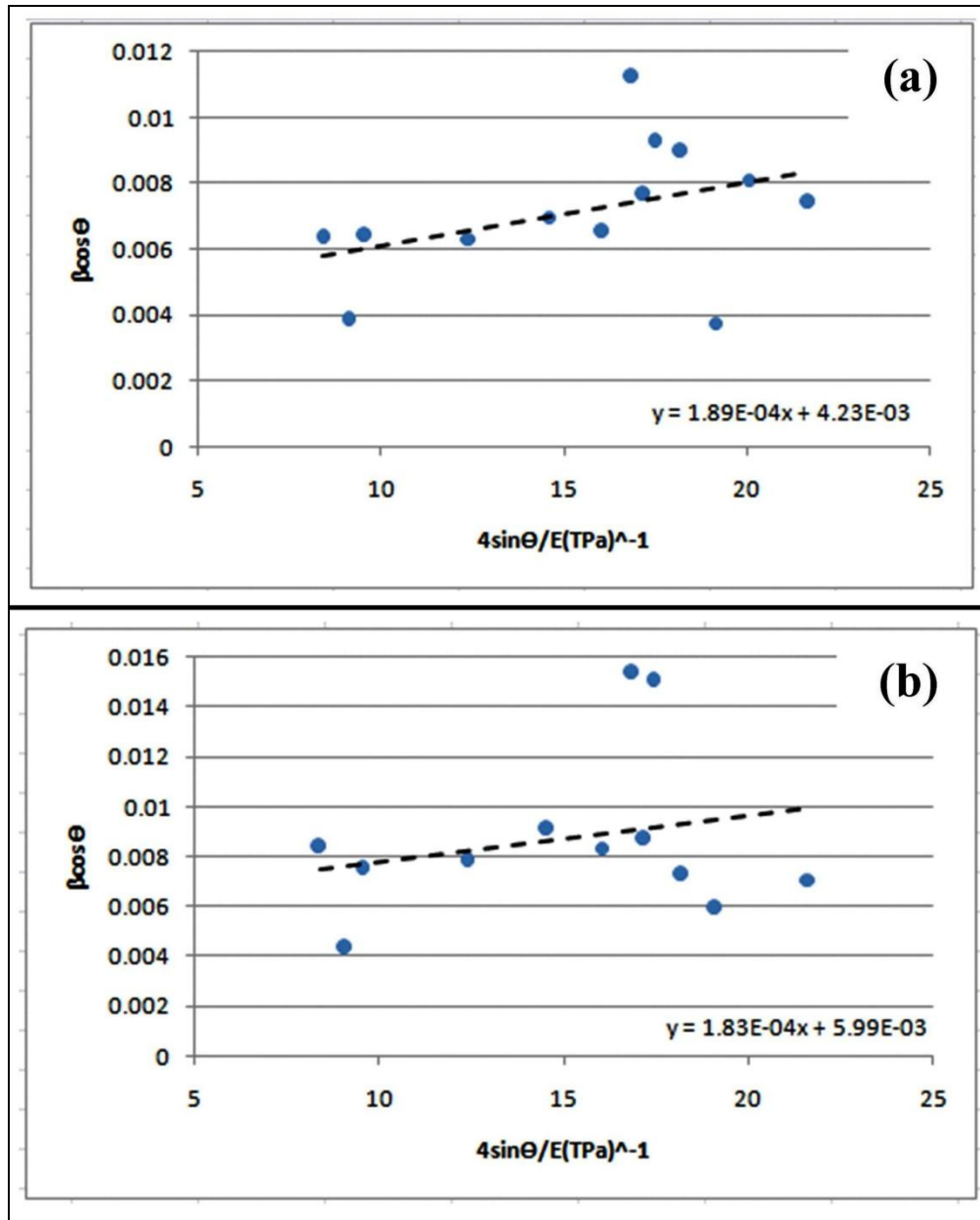


Fig. 3. The modified form of Williamson–Hall analysis for ZnO (a) and ZnO:Mn (b) nanoparticles. Stress is extracted from the slope.

Meantime, the dislocation density ( $\delta$ ) in the sample was determined using the expression [6]:

$$\delta = \frac{1}{D^2} \quad (6)$$

Where the dislocation density ( $\delta$ ) was estimated to be  $2.14 \times 10^{15}$  and  $2.98 \times 10^{15}$  Line/m<sup>2</sup> for ZnO and ZnO:Mn nanoparticles.

**Atomic absorption study**

The atomic absorption studies confirmed attendance of manganese at Zinc sites in ZnO:Mn nanoparticles. It supported the result obtained by XRD analysis. The amount of Mn doping is about 1% by weight.

**Optical study**

For the measurements of UV-Vis spectroscopy, we use the PVP, butanol and water as

microemulsion system and nanoparticles are suspended in the emulsion. The thickness of solution in quartz glass was 1 cm. The optical characteristic of the samples is investigated from the absorption measurements in the range of 300–700 nm. Figure 4 shows the UV–Vis absorption spectra of ZnO and ZnO:Mn nanoparticles. The excitonic absorption peak is observed due to the ZnO and ZnO:Mn nanoparticles at 310 nm, which lies much below the band gap wavelength of 388 nm of bulk ZnO [3].

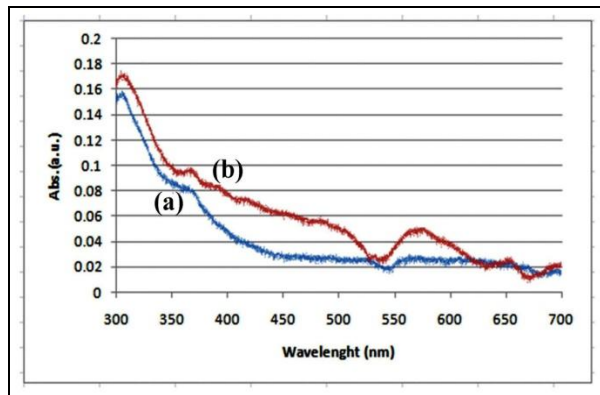


Fig. 4. UV-Vis absorption and transmission characteristics of ZnO (a) and ZnO:Mn (b) nanoparticles.

Absorption coefficient ( $\alpha$ ) associated with the strong absorption region of the sample was calculated from absorbent ( $A$ ) and the sample thickness ( $t$ ) was used the relation:

$$\alpha = 2.3026 \frac{A}{t} \quad (7)$$

While the optical band gap can be calculated using the following relation [6-7]:

$$\alpha h\nu = B(h\nu - E_g)^{0.5} \quad (8)$$

Where  $B$  is a constant and  $E_g$  is the optical band gap of the material. Plot of  $(\alpha h\nu)^2$  vs.  $h\nu$  will indicate a divergence at an energy value. The estimated band gap from the plot of  $(\alpha h\nu)^2$  versus  $h\nu$  for ZnO and ZnO:Mn nanoparticles can be seen in Figure 5. The calculated band gap value of the ZnO and ZnO:Mn were 3.53 and 3.58 eV. The ZnO:Mn nanoparticles band gap values are

lower than ZnO nanoparticles because the magnetic properties of ZnO:Mn nanoparticles increase by doped manganese and interaction potential become more strong in comparison with ZnO nanoparticles [4].

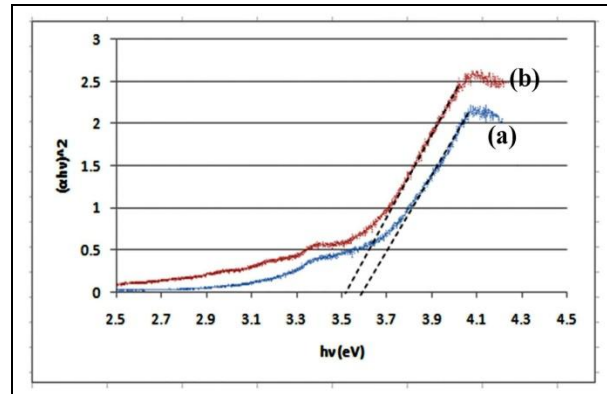


Fig. 5. The plot of  $(\alpha h\nu)^2$  versus  $h\nu$  of ZnO (a) and ZnO:Mn (b) nanoparticles.

#### Photoluminescence study

Room temperature PL spectra of the ZnO and ZnO:Mn nanoparticles samples is shown in Figure 6. The spectra of nanoparticles mainly consist of four emission bands: a strong UV emission band at ~400 and 395 nm, a weak blue band at ~450 and 445 nm, a weak blue–green band at ~490 and 485 nm and a very weak green band at ~530 and 525 nm for ZnO and ZnO:Mn nanoparticles. The strong UV emission corresponds to the exciton recombination related near-band edge emission of ZnO. The weak blue and weak blue–green emissions are possibly due to surface defects in the ZnO nanoparticles as in the case of ZnO nanomaterials reported by other researchers. The weak green band emission corresponds to the singly ionized oxygen vacancy in ZnO, and this emission results from the recombination of a photogenerated hole with the singly ionized charge state of the specific defect [7]. The low intensity of the green emission may be due to the low density of oxygen vacancies during the preparation of the nanoparticles, where as the strong room-temperature UV emission intensity should be attributed to the high purity with perfect crystallinity of the synthesized nanoparticles.

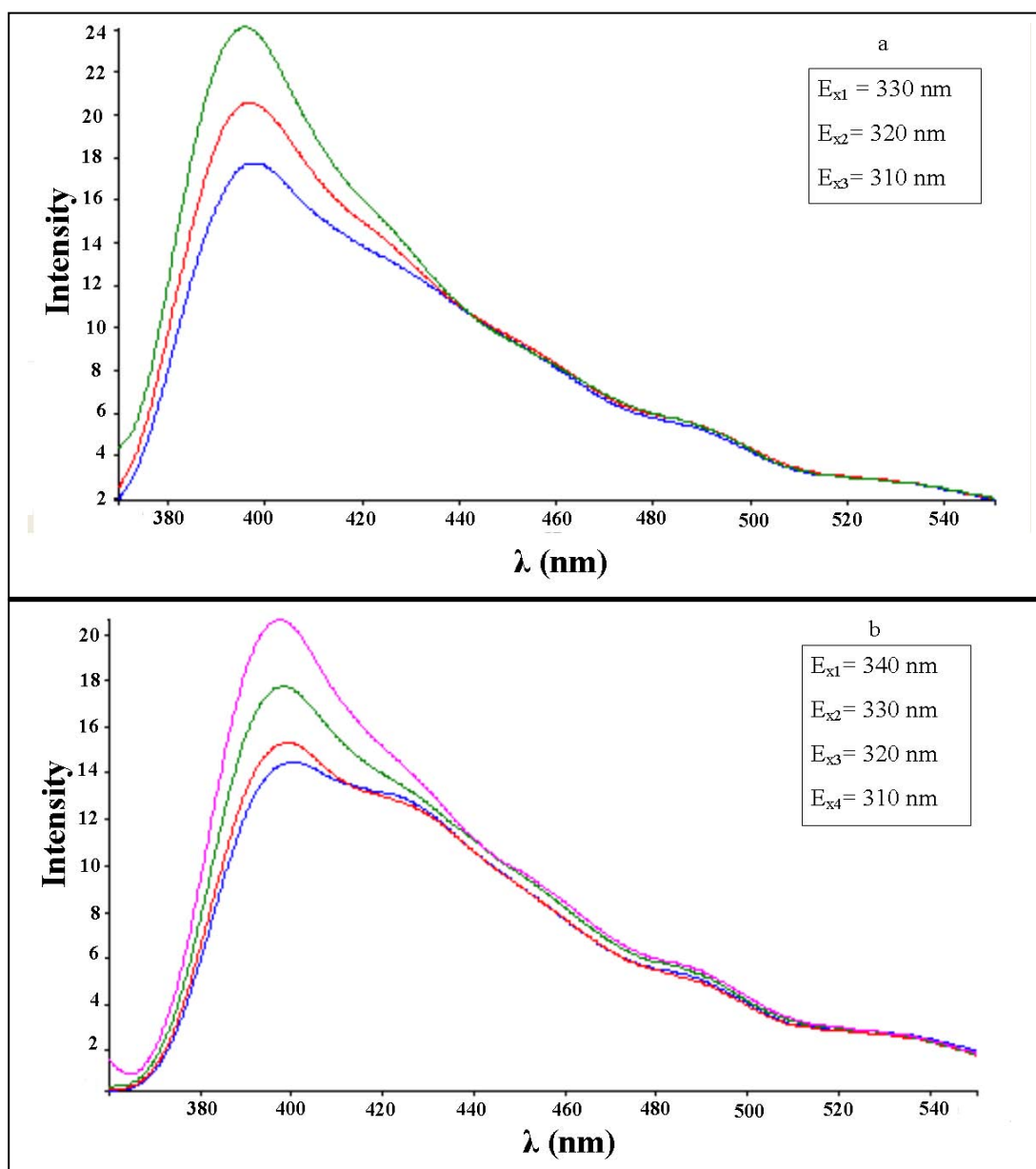


Fig. 6. Room temperature photoluminescence spectra of ZnO (a) and ZnO:Mn (b) nanoparticles.

## CONCLUSION

ZnO and ZnO:Mn nanoparticles with hexagonal structure have been synthesized by the reverse micelle method using PVP as surfactant. The XRD studies of these nanoparticles revealed that their average size is about 21 and 18 nm for ZnO and ZnO:Mn nanoparticles. It can be seen that the highest texture coefficient was in (002) plan for ZnO and ZnO:Mn nanoparticles prepared in this study. The atomic absorption studies confirmed

existence of manganese at Zinc sites in ZnO:Mn nanoparticles. Also, the UV-Vis studies revealed that their optical band gap energy is 3.53 and 3.58 eV for ZnO and ZnO:Mn nanoparticles. Room-temperature photoluminescence spectra of all the samples showed four main emission bands including a strong UV emission band, a weak blue band, a weak blue-green band, and a weak green band which indicated their high structural and optical quality.

**REFERENCES**

- [1] Cruz-Va'zquez C., Bernal R., Burruel-Ibarra S.E., Grijalva-Monteverde H., Barboza-lores M., (2005), Thermoluminescence properties of new ZnO nanophosphors exposed to beta irradiation. *Optical Materials*. 27:1235–1239.
- [2] Kumar D., Kumar S., Bhatti H. S., Gupta A., Sharma J. K., (2008), Synthesis of zno:mn nanoparticles, nanobelts and nanorods. *Journal of Ovonic Research*. 4:101 – 105.
- [3] Kumbhakar P., Singh D., Tiwary C. S., Mitra A. K., (2008), Chemical synthesis and visible photoluminescence emission from monodispersed ZnO nanoparticles. *chalcogenide letters*. 5:387-394.
- [4] Jayakumar O.D., Gopalakrishnan I.K., Kadam R.M., Vinu A., Asthana A., Tyagi A.K., (2007), Magnetization and structural studies of Mn doped ZnO nanoparticles:Prepared by reverse micelle method. *Journal of Crystal Growth*. 300:358–363.
- [5] Khorsand Zak A., Abd. Majid W.H., Abrishami M.E., Yousefi R., (2011), X-ray analysis of ZnO nanoparticles by Williamson-Hall and size-strain plot methods. *Solid State Sciences*. 13:251-256.
- [6] Ilican S., Caglar Y., Caglar M., (2008), Preparation and characterization of ZnO thin films deposited by sol-gel spin coating method. *Journal of optoelectronics and advanced materials*. 10:2578–2583.
- [7] S., Masingboon C., Promarak V., Seraphin S., (2007), Synthesis and optical properties of nanocrystalline V-doped ZnO powders. *Optical Materials*. 29:1700–1705.